RSC Advances

ROYAL SOCIETY OF CHEMISTRY

www.rsc.org/advances

Adsorption of tungstate on kaolinite: adsorption models and kinetics

Li Ruiping, Lin Chunye*, Liu Xitao

State Key Joint Laboratory of Environmental Simulation and Pollution Control, School of Environment, Beijing Normal University, Beijing, China

Abstract: The adsorption characteristic of tungstate onto kaolinite has been studied using batch experiment under ambient temperature. The effect of various operating variables, viz., contact time, initial concentration, solution pH, ionic strength and competitive anion has been investigated. The optimum contact time needed to reach equilibrium was found to be 48 h. Tungstate adsorption isotherms are fitted well by both Langmuir and Freundlich models and the maximal adsorption capacity of the kaolinite sample is 35.54 mmol kg^{-1}. Tungstate adsorption increases at pH range 3-5 and reaches a maximum at average equilibrium pH 4.24, but decreases from 83.7% to 10.6% with the pH increasing from 5.35 to 11.03. Tungstate adsorption increases from 71.9% to 89.4% with ionic strength ranging from 0.001 M to 0.1 M NaCl. With the increase of the mol ratio P/W from 0 to 10, tungstate adsorption decreases from 24.38 mmol kg^{-1} to 21.61 mmol kg^{-1}, while phosphate adsorption increases from -2.09 mmol kg^{-1} to 27.45 mmol kg^{-1}. These results demonstrate that tungstate might be adsorbed onto the tungstate-specific adsorption sites of the kaolinite minerals mainly via inner-sphere complexation.

Keywords: Tungstate, kaolinite, adsorption, kinetic, isotherm

1. Introduction

Tungsten is a transition metal and has increased interest due to the scrutiny of a children

State Key Joint Laboratory of Environmental Simulation and Pollution Control, School of Environment, Beijing Normal University, Beijing 100875, China
*Corresponding author: Tel: +10 58801858, Fax: +86 10 58801858, email: c.lin@bnu.edu.cn

leukemia cluster in Fallon, NV, and suspected cases in Sierra Vista, AZ and Elk Grove, CA (Seiler et al., 2005; Koutsospyros et al., 2006; Sheppard et al., 2006). Anthropogenic activities significantly increase tungsten release in environmental systems such as W mining and smelting, military combat/training operations, agrochemical practices including the application of W-containing fertilizers, and non-sustainable disposal of W-containing substances (e.g. disposal of light bulbs in landfills and land application of wastewater residuals) (Strigul et al., 2005; Sheppard et al., 2006).Tungsten metal in natural persists primarily as the tungstate anion and is thermodynamically stable in environment (Gustafsson, 2003; Seiler et al., 2005; Strigul et al., 2005; Koutsospyros et al., 2006).

Only very few adsorption studies of tungstate on natural sorbents have been reported to date (Gustafsson, 2003; Xu et al., 2009; Tuna et al., 2012; Tuna and Braida, 2014). Further, these studies mainly focused on tungstate adsorption on iron oxides/hydroxides and demonstrated that tungstate can strongly bind to iron oxides/hydroxides, pH had a strong influence on tungstate adsorption and phosphate has a comparable competitive effect on tungstate adsorption (Gustafsson, 2003; Xu et al., 2006; Xu et al., 2009). Kaolinite is the most abundant mineral in soil and sediments (Chen et al., 2000) and has received considerable recognition as a natural scavenger because of its high adsorption capacity. However, studies reported the adsorption of tungstate on kaolinite was scarce (Tuna et al., 2012; Tuna and Braida, 2014).

China is the world's largest W producer and consumer. Ganzhou in the south of Jiangxi province, being the birth place of Chinese W industry, is extremely rich in W source. So Ganzhou is called as “Tungsten capital of the world”. There are three major tungsten mines: Xihuashan, Dangping, and Piaotang, among which Xihuashan is the first tungsten mine operated in China. It is

believed that tungsten pollution from tungstate mining and smelting activities is very severe, resulting in significant environmental problems in China (Li et al., 2014). However, the existing knowledge base does not provide clear information about the fate of tungsten in the environment. Therefore, it is essential to understand tungstate adsorption/desorption and quantify the maximal tungstate adsorption capacity on kaolinite. In addition, the knowledge on tungstate adsorption/desorption on kaolinite is lacking and thus would be interesting to worldwide scientists.

The purpose of this study is to elucidate the role of pH, ionic strength and competitive anion (PO_4^{3-}) on tungstate adsorption onto kaolinite surface. Adsorption data has been analyzed with the help of adsorption models to determine the adsorption constants and obtain thermodynamic parameters associated with the adsorption process.

2. Materials and methods

2.1 Regents and Materials

All chemicals used in the study were of analytical grade or higher. All solutions were prepared with double distilled water and all polypropylene centrifuge tubes were cleaned by soaking in 10% HNO_3 and rinsed with deionized water. All experiments were performed in duplicate.

The kaolinite used in this study was obtained from Beijing Mengyimei Bio-Tech Co., Ltd (Beijing, China). The specific surface area of the kaolinite was measured by the Model QS-7 Quantasorb surface area analyzer (Quantachrom Co., Greenvale, NY). The X-ray diffraction (XRD) pattern of the kaolinite was obtained using a X'Pert PRO MPD instrument (PANalytical B.V.， Netherlands) with filtered Cu Kα radiation (n=0.1548 nm) operated at 40 kV and 40 mA. The kaolinite sample also was characterized using S4800 scanning electron microscope.

2.2 Adsorption experiments

2.2.1 Kinetic studies

The kinetic studies were conducted to examine the influence of time on the adsorption of tungstate on kaolinite in 0.1 M NaCl at pH 5.0. Batch method was used to examine the effect of time on the adsorption by shaking kaolinite suspensions in a series of 50 mL polypropylene centrifuge tubes containing 500 mg of kaolinite in 25 mL of 50 mg L^{-1} WO_4^{2-} ($Na_2WO_4 \cdot 2H_2O$) for 1, 2, 4, 8, 12, 24, 36 ,48 and 60 h. At the designed time, the tubes were centrifuged at 8000 rpm for 20 min using Xiang Yi centrifuge (H-1650, China) to separate the solid from liquid phases followed by filtering with 0.45 μm filter.

2.2.2 Adsorption isotherms

The influence of the initial WO_4^{2-} concentration was determined in 0.1 M NaCl at pH 5.0. The tests were run with initial WO_4^{2-} concentration ranging from 1 to 300 mg L^{-1} at 25 ± 1℃ in order to calculate the thermodynamic parameters of the absorption reaction.

2.2.3 Adsorption of tungstate as a function of pH and ionic strength

Batch adsorption of WO_4^{2-} at different pH and ionic strength was examined by shaking kaolinite suspensions in 50 mL polypropylene centrifuge tubes containing 500 mg of kaolinite in 25 mL of 100 mg L^{-1} WO_4^{2-} for 48 h. Suspension pH was maintained throughout the experiment using dilute HCl and NaOH solutions. Ionic strength was maintained by adding various concentration of NaCl solution. After the 48 h reaction period, the tubes were centrifuged and filtered.

2.2.4 Competitive anion

The influence of competitive anion (PO_4^{3-}) ($NaH_2PO_4 \cdot 2H_2O$) on WO_4^{2-} adsorption was investigated by simultaneously adding WO_4^{2-} and PO_4^{3-} stock solutions to sorbent suspension. The mol concentration ratio (P/W) was in the range of 0.1, 0.5, 1, 5 and 10.

2.2.5 Analytical methods

The pH of the solutions was measured using a basic PB-10 pH meter (Sartorius, Germany), calibrated using commercial pH 4.01, 6.86 and 9.18 buffers. The concentration of W and P in the supernatants was measured with ICP MS (X Series II, Thermo Electron) and ICP AES (SPECTRO ARCOS EOP, SPECTRO Analytical Instruments GmbH).

3. Results and discussion

3.1. Characterization of the kaolinite

The X-ray diffraction spectrograph of the kaolinite clay was shown in Fig. 1. The structure of the kaolinite clay is given as $Al_2(Si_2O_5)(OH)_4$ by XRD and mainly consists of kaolinite and quartz. SEM image of kaolinite sample (Fig. 2.) demonstrates that kaolinite is mainly composed of flakes, which is agreement with the microscopic observation of kaolinite reported. The specific surface area of the kaolinite clay was found to be 15.8 m^2/g determined by BET method using N_2.

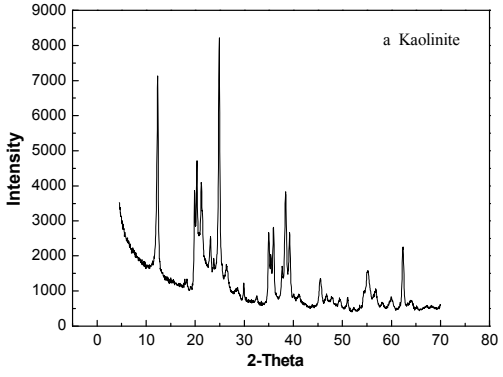

Fig. 1. The XRD pattern of kaolinite clay.

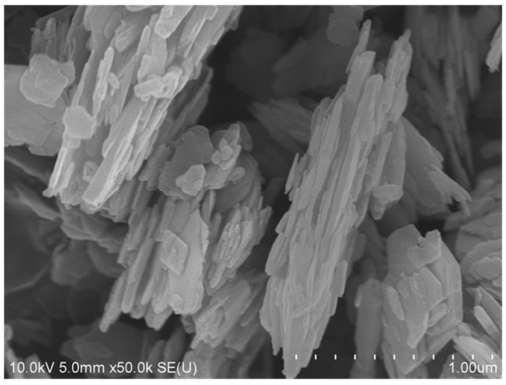

Fig. 2. SEM micrograph of kaolinite clay.

3.2. Effect of contact time

The plot of WO_4^{2-} adsorption on kaolinite with different contact times at a pH value of 5.0 is shown in Fig. 3. The adsorption of WO_4^{2-} occurred very quickly during the first 12 h, then the remaining concentration of WO_4^{2-} becomes asymptotic to the time axis, such that there is no

105 appreciable change in the remaining concentration after 48 h. This time is presumed to represent the
106 equilibrium time at which an equilibrium concentration is presumed to have been attained. All the
107 further experiments were conducted for 48 h.

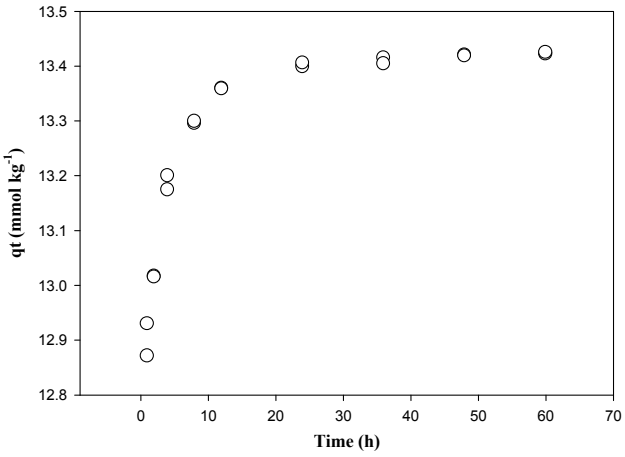

108

109 Fig. 3. Adsorption of tungstate onto kaolinite clay as a function of contact time, with reaction condition: ionic
110 strength (*I*) =0.1 M NaCl, pH =5.0±0.1, T=298±1K, initial concentration (WO_4^{2-}) =0.27 mM.

111 To analyze the rate constants of tungstate adsorption on kaolinite, Lagergren first-order rate
112 expression (Lagergren, 1898) and pseudo-second-order rate expression (Veli and Alyuz, 2007)
113 (Eq.(1) and Eq.(2)) were used to simulate the kinetic adsorption data:

114 $$log(q_e - q) = logq_e - \frac{k_{ad}}{2.303}t \qquad (1)$$

115 $$\frac{t}{q} = \frac{1}{k_2 q_e^2} + \frac{1}{q_e}t \qquad (2)$$

116 where q and q_e are amounts of WO_4^{2-} adsorbed (mmol kg^{-1}) at time, t (h) and at equilibrium,
117 respectively and k_{ad} is the Lagergren rate constant for tungstate adsorption (1/h). where k_2 is the
118 pseudo-second-order rate constant (kg $mmol^{-1}$ h^{-1}).

119 The straight line plot of log (q_e- q) versus t (Fig. 4a) indicate the applicability of the above
120 equation. Value of k_{ad} calculated from the slope of the linear plot was determined to be 1.05×10^{-2}

h^{-1}, which is consisted with tungstate adsorption onto Oxisols (k_{ad} 1.10×10^{-2} h^{-1} at the initial tungstate concentration 0.04 mM) (Li et al., 2014). The straight line plot of t/qt versus t (Fig. 4b) indicate that the kinetics of WO_4^{2-} adsorption on kaolinite can be well described by the pseudo-second order rate equation (R^2=1).

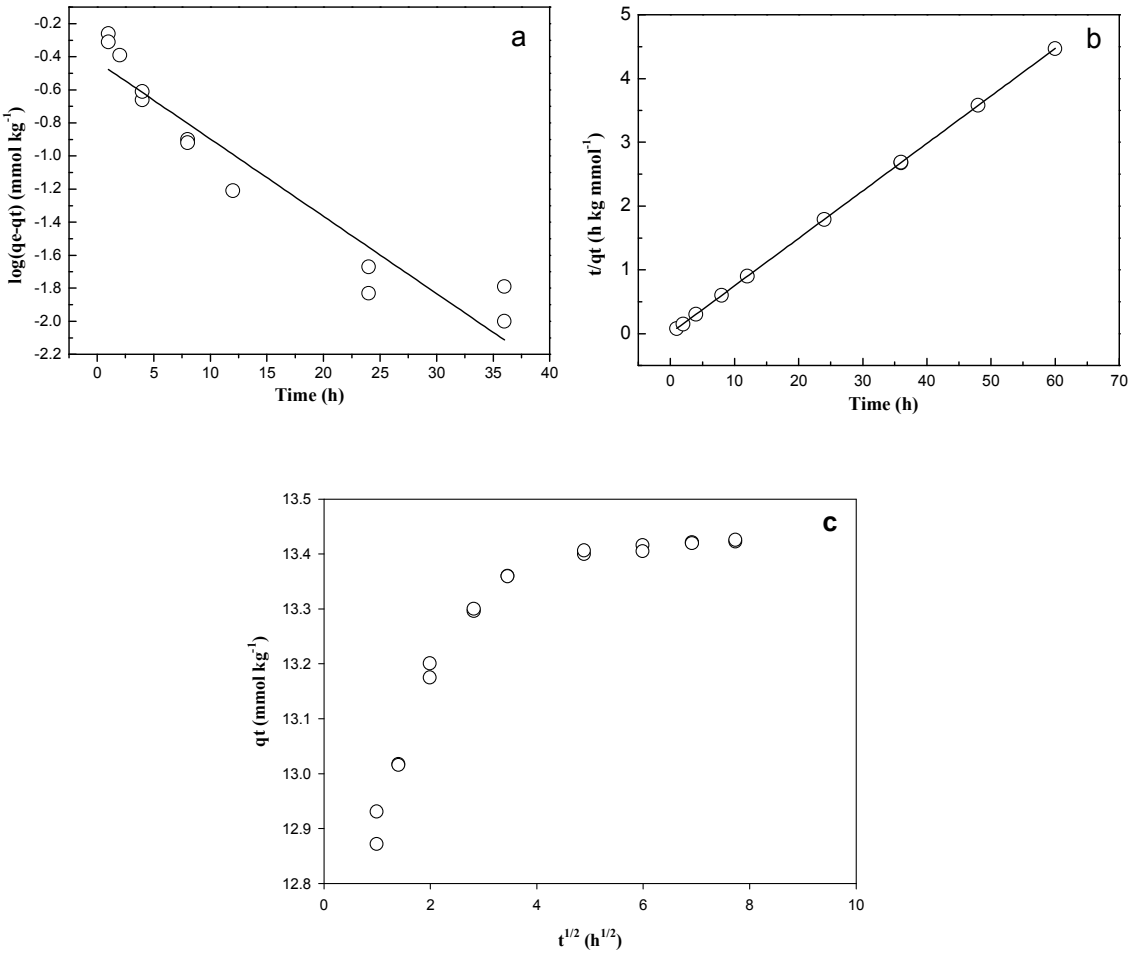

Fig. 4. Kinetic simulation of tungstate adsorption onto kaolinite: (a) pseudo-first order model, (b) pseudo-second order model, (c) intraparticle diffusion model.

To further discuss the rate of internal mass transfer, the adsorption data was fitted to the intraparticle diffusion model given by Weber and Morris (1963) (Eq. (3)):

$$q = k_{id}t^{1/2} \quad (3)$$

where k_{id} is the relevant rate constant (mmol kg^{-1} $h^{1/2}$). Plot of tungstate adsorbed, q versus $t^{1/2}$,

is presented in Fig. 4c. The plot follows three phases, initial curved portion followed by linear and a plateau. The initial curved portion is attributed to the bulk diffusion, the linear portion to the intraparticle diffusion and the plateau to the equilibrium. The features of plot indicate that transport of WO_4^{2-} from the solution through the particle solution interface, into the pores of the particles as well as the adsorption on the available surface of kaolinite, are both responsible for the uptake of WO_4^{2-}. The deviation of the curves from the origin also indicates that intraparticle transport is not the only rate limiting step. The value of rate constants (k_{id}) was obtained from the slope of the linear portion of the curve was 0.185 mmol kg^{-1} $h^{1/2}$.

3.3. Adsorption isotherm

The adsorption isotherms of tungstate are shown in Fig. 5. The adsorption isotherm plot illustrated linear distribution in the range 0-1.63 mmol L^{-1}. Further, for the same equilibration time, the adsorption of tungstate is higher for greater values of initial concentration of tungstate anion and decreases with increasing initial concentration. This may be due to the limited total available adsorption sites for a fixed adsorbent dose.

The adsorption models have been used to determine the mechanistic parameters associated with the adsorption process. In this study, The Langmuir model and Freundlich model were applied to evaluate the WO_4^{2-} adsorption isotherm data.

The Langmuir model has the form (Langmuir, 1918) :

$$\frac{C_e}{q_e} = \frac{C_e}{q_m} + \frac{1}{q_m K_L} \qquad (4)$$

where *Ce* is the equilibrium concentration of tungstate in solution, q_e is the tungstate adsorption amount, q_m is maximal adsorption capacity, and K_L (L $mmol^{-1}$) is a constant related to the binding energy.

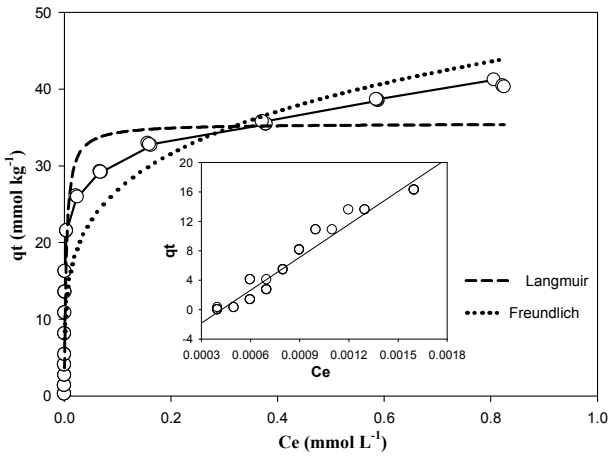

Fig. 5. Adsorption isotherm plot for the adsorption of tungstate onto kaolinite clay.

The Freundlich model has the general form:

$$q_e = K_F C^{1/n} \quad (5)$$

where *Ce* is the equilibrium concentration of tungstate in solution, q_e is the amount of tungstate adsorption, and K_F (mmol^{1-n} kg^{-1} L^n) and *n* are Freundlich constants related to the adsorption intensity and adsorption capacity.

Table 1. Parameters of Langmuir and Freundlich models**.**

Model	K_L (L mmol^{-1})	Q_{max} (mmol kg^{-1})	K_F mmol^{1-n} kg^{-1} L^n	n	R^2	SE
Langmuir	0.0035	35.54	---	---	0.94	3.65
Freundlich	---	---	45.92	4.30	0.87	5.40

Table 1 lists the isothermal parameters for tungstate adsorption on kaolinite based on the simulated of experiment data as shown in Fig. 5. Based on the correlating coefficients, the Langmuir model was found to fit the test data better than Freundlich model. The maximal adsorption tungstate capacity calculated from Langmuir model is 35.54 mmol kg^{-1}, and the Langmuir equilibrium constant K_L, had a value of 0.0035 L mmol^{-1}. This results are in agreement

168 with the previous research reported by Tuna et al. (2012). Tuna et al. investigated the tungsten
169 adsorption from canister rounder munitions onto natural kaolinite. They found that tungsten
170 adsorption on natural kaolinite was fitted best by Langmuir model and the maximal tungsten
171 adsorption capacity was 8.28 mmol kg^{-1}. The larger difference observed for tungstate maximal
172 adsorption capacity is likely related to the impurity of the natural kaolinite used in the Tuna et al.
173 study. Our another research found that the maximal capacity of tungstate adsorption onto the
174 Oxisols was also fitted best by both the Langmuir model and the Freundlich model, with the
175 maximal capacity of 10.09 mmol kg^{-1} and the distribution coefficient 12.6 L g^{-1} (Li et al., 2014). Xu
176 et al. (2009) found that the maximal capacity of tungstate adsorption onto goethite was much higher
177 than its on kaolinite with the maximal capacity of 225.7 mmol kg^{-1} and the distribution coefficient
178 159.1 L g^{-1}. This difference is duo to the characteristic of the different adsorbent. Therefore, the
179 maximal tungstate adsorption capacity onto kaolinite is higher than Oxisols, but much lower than
180 that for goethite.

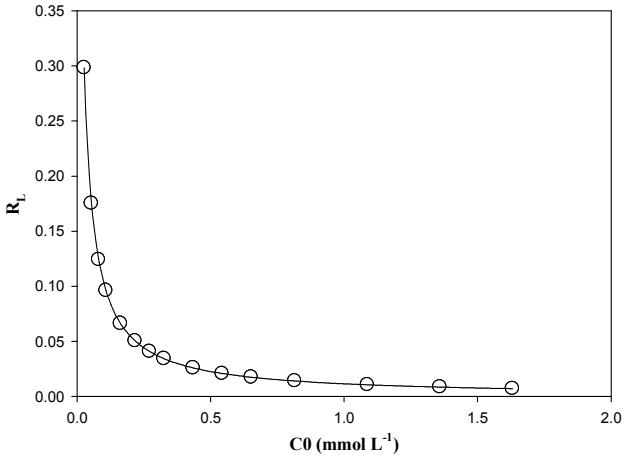

181

182 Fig. 6. Variation of adsorption intensity (R_L) with initial tungstate concentration.

183 According to Hall et al., (1966) and Sari et al., (2007), the essential features of the Langmuir

isotherm can be expressed in terms of a dimensionless constant separation factor or equilibrium parameter R_L, which is defined by the following relationship (Eq.(6)):

$$R_L = \frac{1}{1+K_L C_0} \qquad (6)$$

where C_0 (mmol L^{-1}) is the initial amount of tungstate. The R_L parameter is considered as more reliable indicator of the adsorption. There are four probabilities for the R_L value:(i) for favorable adsorption, $0 < R_L < 1$, (ii) for unfavorable adsorption, $R_L > 1$, (iii) for linear adsorption, $R_L = 1$, and (iv) for irreversible adsorption, $R_L = 0$. The value of R_L for tungstate adsorption onto kaolinite ranges from 0.007 to 0.298 between 0.08 and 1.63 mmol L^{-1} and approaches zero with increase in the C_0 value (Fig. 6). This parameter ($0 < R_L < 1$) indicates that the kaolinite clay is a suitable adsorbent for the adsorption of tungstate from aqueous solution.

3.4. Effect of pH

The adsorption of tungstate (WO_4^{2-}) on kaolinite as a function of pH from 3 to 11 is illustrated by Fig. 7. The adsorption of tungstate increases at pH range 3-5 and reaches a maximum at average equilibrium pH 4.24(equilibrium pH 4.35, 4.16, 4.21, respectively); but the adsorption of tungstate on kaolinite decreases significantly from 83.7% to 16.7% at pH 5-7, then it decreases very slowly to approximately 11% at pH ＞7. The effect of pH on the tungstate adsorption onto the kaolinite is consistent with Tuna and Braida (2014) results. Tuna and Braida found that maximum adsorption of tungstate on natural kaolinite is at pH 3 (87%) and adsorption decreases slowly in the 6-10 pH range. The similar pH-dependence curve of tungstate adsorption on iron oxide has been reported by Xu et al. (2006). They found that tungstate has a broad adsorption envelope onto goethite across a wide pH range, with the maximum adsorption below pH 5.1, and only 10% above pH 10 on the goethite surface. These results may be explained by the findings of Hingston et al. (1971), who

concluded that adsorption for anions of weak acids is the strongest at pH values near their acid dissociation constants (pK_a). The two pKa values for H_2WO_4 (pK_{a1} = 3.62, (Wesolowski et al., 1984); pK_{a2} =5.08, (Wood and Samson, 2000)) bracket a wider pH range where the maximum adsorption of WO_4^{2-} on kaolinite occurs. On the other hand, the solution pH affects the tungstate speciation which relates to its adsorption mechanism on kaolinite. Tungstate speciation is complex and tends to polymerize to form some insoluble isopolytungstate under acidic conditions such as $[HW_6O_{12}]^{-3}/[H_2W_6O_4]^{-6}$ at pH=4.0, $[W_2O(OH)_8]^{+2}/[W_2O_4(OH)]^{-3}$ at pH=6.0. So there may be more than one mechanism for tungstate adsorption onto kaolinite: i.e. adsorption and polymerization at low pH. Tungstate occurs in the forms of $WO_4^{-2}/W(OH)_8^{-2}$ only when pH＞6.2. The decreasing trend of tungstate adsorption on kaolinite with increasing pH may be explained that the high negatively charged surface sites of kaolinite with increasing pH did not favor the adsorption of tungstate due to electrostatic repulsion. Also, an abundance of OH^- ions in basic solution creates a competitive environment with anionic ions of tungstate for the adsorption sites causing a decrease of adsorption.

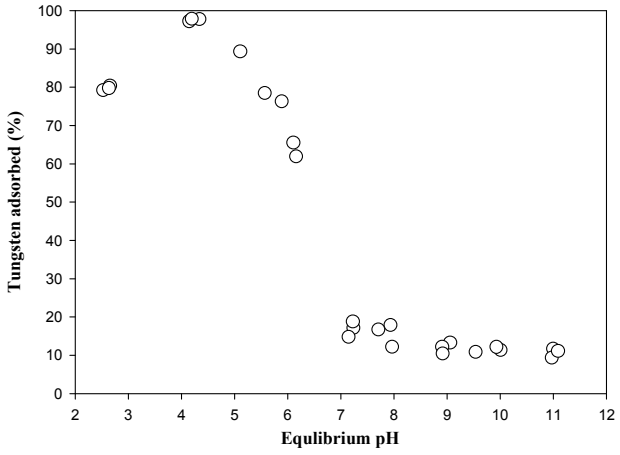

Fig. 7. Effect of pH on the adsorption of tungstate onto the kaolinite clay.

3.5. Effect of ionic strength

Fig.8 shows the effect of ionic strength on the adsorption of tungstate onto kaolinite clay. It was observed that tungstate adsorption increased from 71.9% to 89.4% with ionic strength ranging from 0.001 M to 0.1 M NaCl. It is possible to distinguish between inner-sphere and outer-sphere anion surface complexes by studying the effects of ionic strength on anion partitioning, and hence, to get some useful information about the adsorption mechanism (Hayes et al., 1988; McBride, 1997; Sparks, 2003; Goldberg, 2005). Adsorption behavior that is respond to higher ionic strength with greater adsorption is macroscopic evidence for inner-sphere complexation. McBride (1997) indicated that higher ionic strength might lead to the transform of adsorbate from outer-sphere complex to inner-sphere complex and hence might increase overall adsorption. The similar adsorption trend was reported for borate and arsenate (Goldberg et al., 1993; Deliyanni et al., 2003; Payne and Abdel-Fattah, 2005).Thus, the increase of ionic strength might lead to the formation of the more tungstate inner-sphere complex onto the clay colloids and thus increased the overall tungstate adsorption onto them.

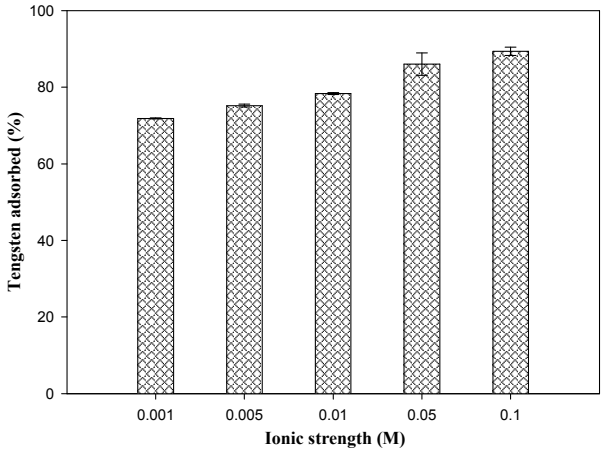

Fig. 8. Effect of ionic strength on the adsorption of tungstate onto the kaolinite clay.

3.6. Effect of competitive anions

Competitive anions greatly affect the mobility and bioavailability of tungstate in environment. The effect of the presence of PO_4^{3-} on the amount of WO_4^{2-} adsorbed on kaolinite was designed in which initial tungstate concentration was 0.5 mM, while initial phosphate concentration ranged from 0.05 to 5.0 mM (Fig. 9). With the increase of the mol ratio P/W from 0 to 10, tungstate adsorption decreased from 24.38 mmol kg^{-1} to 21.61 mmol kg^{-1}, while phosphate adsorption increased from -2.09 mmol kg^{-1} to 27.45 mmol kg^{-1} (Fig. 9). As shown in Fig. 9, the decrease in the amount of tungstate adsorbed on kaolinite as the ratio P/W increases , is less than the increase in the amount of phosphate adsorbed. This observation must arise from some adsorption taking place without displacement of tungstate. Mulcahy et al. (1990) concluded that tungstate adsorbed on two types of surface sites of alumina, producing loosely and tightly bound surface species. Therefore, it can be concluded that the kaolinite might have small adsorption sites common to tungstate and phosphate anions and large adsorption sites specific to tungstate or phosphate anions.

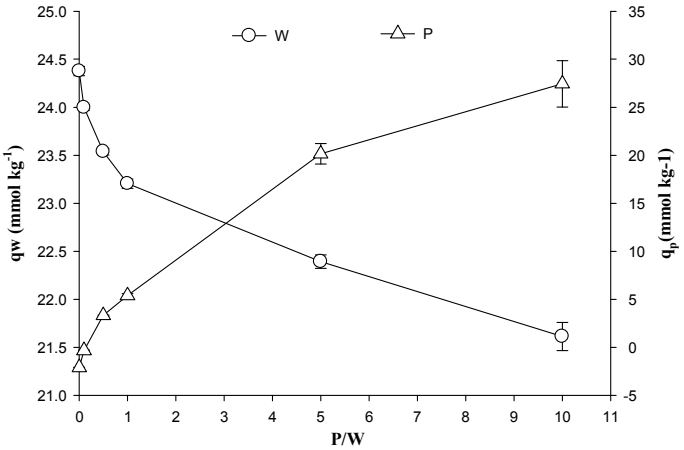

Fig. 9. Effect of PO_4^{3-} at various concentrations on the adsorption of tungstate with the reaction conditions: pH = 5.0±0.5, initial tungstate concentration =0.5 mM, reaction time = 48 h, and T= T=298±1K.

4. Conclusion

In this study，the adsorption of tungstate on purity kaolinite was discussed for the first time and the effect of contact time, initial concentration, pH, ionic strength and competitive anion was examined. Tungstate adsorption onto purity kaolinite generally reached equilibrium after 48 h. The adsorption isotherms can be well described with both Langmuir model and Freundlich model. Tungstate adsorption increases at pH range 3-5 and decreases significantly at pH ＞7, while it markedly increased with the increase of ionic strength from 0.001 M to 0.1 M NaCl. With the increase of phosphate concentration from 0.05 mM to 5.0 mM, tungstate adsorption slightly decreased from 24.38 mmol kg^{-1} to 21.61 mmol kg^{-1}. These results demonstrate that tungstate might be adsorbed onto the tungstate-specific adsorption sites of the kaolinite clay mainly via inner-sphere complexation. The results clearly show that the adsorption of tungstate on kaolinite play an important role in determining the fate and transformation of tungstate in natural environments. Spectroscopic study on the microstructure of tungstate may be necessary to identify the species of tungstate on kaolinite surface in future.

Acknowledgements

This study was supported by the National Natural Science Foundation of China (41371441) and the Ministry of Environmental Protection Funded Project (201309044).

Reference

Chen, J., Anandarajah, A., Inyang, H., 2000. Pore fluid properties and compressibility of kaolinite. Journal of Geotechnical and Geoenvironmental Engineering, 126, 798-807.

Deliyanni, E. A., Bakoyannakis, D. N., Zouboulis, A. I., Matis, K. A., 2003. Sorption of As (V) ions by akaganeite-type nanocrystals. Chemosphere, 50, 155-163.

276 Goldberg, S., 2005. Inconsistency in the triple layer model description of ionic strength dependent
277 boron adsorption. Journal of colloid and interface science, 285, 509-517.
278 Goldberg, S., Forster, H. S., Heick, E. L., 1993. Boron adsorption mechanisms on oxides, clay
279 minerals, and soils inferred from ionic strength effects. Soil Science Society of America
280 Journal, 57, 704-708.
281 Gustafsson, J. P., 2003. Modelling molybdate and tungstate adsorption to ferrihydrite. Chemical
282 Geology, 200, 105-115.
283 Hall, K. R., Eagleton, L. C., Acrivos, A., Vermeulen, T., 1966. Pore-and solid-diffusion kinetics in
284 fixed-bed adsorption under constant-pattern conditions. Industrial & Engineering Chemistry
285 Fundamentals, 5, 212-223.
286 Hayes, K. F., Papelis, C., Leckie, J. O., 1988. Modeling ionic strength effects on anion adsorption at
287 hydrous oxide/solution interfaces. Journal of Colloid and Interface Science, 125, 717-726.
288 Hingston, F. J., Posner, A. M., Quirk, J. P., 1971. Competitive adsorption of negatively charged
289 ligands on oxide surfaces. Discussions of the Faraday Society, 52, 334-342.
290 Koutsospyros, A., Braida, W., Christodoulatos, C., Dermatas, D., Strigul, N., 2006. A review of
291 tungsten: from environmental obscurity to scrutiny. Journal of Hazardous Materials, 136, 1-19.
292 Lagergren, S., 1898. About the theory of so-called adsorption of soluble substances.
293 Langmuir, I., 1918. The adsorption of gases on plane surfaces of glass, mica and platinum. Journal
294 of the American Chemical society, 40, 1361-1403.
295 Li, R. P., Luan, R. N., Lin, C. Y., Jiao, D. Q., Guo, B. B., 2014. Tungstate adsorption onto oxisols in
296 the vicinity of the world's largest and longest-operating tungsten mine in China. RSC Advance,
297 4, 63875-63881.

298 McBride, M. B., 1997. A critique of diffuse double layer models applied to colloid and surface
299 chemistry. Clays and Clay minerals, 45, 598-608.
300 Mulcahy F. M., Fay M. J., Proctor, A., Houalla, M., Hercules, D. M., 1990. The adsorption of metal
301 oxyanions on alumina. Journal of Catalysis, 124, 231-240.
302 Payne, K. B., Abdel-Fattah, T. M., 2005. Adsorption of arsenate and arsenite by iron-treated
303 activated carbon and zeolites: effects of pH, temperature, and ionic strength. Journal of
304 Environmental Science and Health, 40, 723-749.
305 Sari, A., Tuzen, M., Citak, D., Soylak, M., 2007. Equilibrium, kinetic and thermodynamic studies of
306 adsorption of Pb(II) from aqueous solution onto Turkish kaolinite clay. Journal of Hazardous
307 Materials, 149, 283-291.
308 Seiler, R. L., Stollenwerk, K. G., Garbarino, J. R., 2005. Factors controlling tungsten concentrations
309 in ground water, Carson Desert, Nevada. Applied Geochemistry, 20, 423-441.
310 Sheppard, P. R., Ridenour, G., Speakman, R. J., Witten, M.L., 2006. Elevated tungsten and cobalt in
311 airborne particulates in Fallon, Nevada: possible implications for the childhood leukemia
312 cluster. Applied Geochemistry, 21, 152-165.
313 Sparks, D. L., 2003. Environmental soil chemistry. Academic press.
314 Strigul, N., Koutsospyros, A., Arienti, P., Christodoulatos, C., Dermatas, D., Braida, W., 2005.
315 Effects of tungsten on environmental systems. Chemosphere, 61, 248-258.
316 Tuna, G. S., Braida, W., Ogundipe, A., Strickland, D., 2012. Assessing tungsten transport in the
317 vadose zone: From dissolution studies to soil columns. Chemosphere, 86, 1001-1007.
318 Tuna, G. S., Braida, W., 2014. Evaluation of the Adsorption of Mono-and Polytungstates onto
319 Different Types of Clay Minerals and Pahokee Peat. Soil and Sediment Contamination: An

International Journal, 23, 838-849.

Veli, S., Alyuz, B., 2007. Adsorption of copper and zinc from aqueous solutions by using natural clay. Journal of hazardous materials , 149, 226-233.

Weber, W. J., Morris, J. C., 1963. Kinetics of adsorption on carbon from solution. Journal of the Sanitary Engineering Division, 89, 31-60.

Wesolowski, D., Drummond, S. E., Mesmer, R. E., Ohmoto, H., 1984. Hydrolysis equilibria of tungsten (VI) in aqueous sodium chloride solutions to 300. degree. C. Inorganic Chemistry, 23, 1120-1132.

Wood, S.A., Samson, I.M., 2000. The hydrothermal geochemistry of tungsten in granitoid environments: I. Relative solubilities of ferberite and scheelite as a function of T, P, pH, and mNaCl. Economic Geology, 95, 143-182.

Xu, N., Christodoulatos, C., Braida, W., 2006. Modeling the competitive effect of phosphate, sulfate, silicate, and tungstate anions on the adsorption of molybdate onto goethite. Chemosphere, 64, 1325-1333.

Xu, N., Christodoulatos, C., Koutsospyros, A., Braida, W., 2009. Competitive sorption of tungstate, molybdate and phosphate mixtures onto goethite. Land Contamination & Reclamation, 17, 45-57.

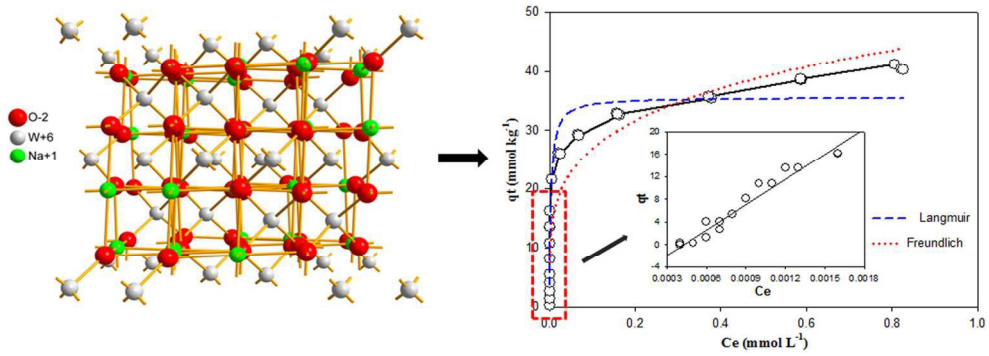

129x50mm (300 x 300 DPI)